Resonant Oscillations Between the Solid Earth and the Atmosphere

Kiwamu Nishida,[1] Naoki Kobayashi,[2] Yoshio Fukao[1]

Continuously excited free oscillations of the whole Earth have been found in the ground noise in a frequency band of long-period surface waves. Here we report evidence of an annual variation of this phenomenon, indicating that the excitation source is not within the solid Earth. There is evidence that these seismic free oscillations resonate with acoustic free oscillations of the atmosphere. The observed amplitudes suggest that the excitation source is at or just above Earth's surface.

Earth's background free oscillations have now been firmly established (*1–4*). They comprise the fundamental spheroidal modes, with amplitudes on the order of 0.5 nanogalileo (nGal) (1 nGal = 10^{-11} m s^{-2}) with little frequency dependence. The cumulative effects of many small earthquakes are too small to explain these amplitudes (*2–5*). Statistical examination of the excited normal modes indicates that these oscillations must be excited randomly and persistently by sources that are distributed globally, with correlation lengths shorter than 600 km (*5*). All of these observations suggest that either atmospheric or oceanic disturbance may be a source of this phenomenon. A dimensional analysis (*4, 6*) has indicated that atmospheric disturbance can generate Earth's free oscillations at a nGal level with a possible annual variation of intensities on the order of 10%. Here we present evidence of an annual variation, which rules out the possibility of excitation sources within the solid Earth. We also report the evidence of the background free oscillations being resonant between the solid Earth and the atmosphere.

We analyzed continuous 10-s sampling records from a period from 1989 to 1998 through a very-long-period high-gain (VH) channel from the vertical STS-1 seismometers at 17 IRIS (Incorporated Research Institution for Seismology) stations (*7*) and 8 GEOSCOPE (*8*) stations (*9*) at the lowest ground noise level (slightly less than 10^{-18} m^2 s^{-3}). For each station, we removed glitches and divided the whole record into 1-day segments with an overlap of 3 hours with the next day. Each of the 1-day segments was Fourier-transformed to obtain the power spectrum. The spectrum might have been disturbed by transient phenomena such as earthquakes and local nonstationary ground or instrumental noise. We calculated the mean power spectral density (PSD) in the mHz band to measure the intensities of such disturbances. Earthquakes with moments greater than 10^{18} newton meters can disturb the spectra (*2–5*). The mean PSDs of earthquake-disturbed segments decay exponentially over time because of Earth's anelasticity. All the seismically disturbed segments with the mean PSDs greater than 1×10^{-18} m^2 s^{-3} were discarded (*5*). We also discarded noisy segments whose mean PSDs were greater than 3.0×10^{-18} m^2 s^{-3}. The remaining segments were considered to be free from the effects of earthquakes and local nonstationary ground or instrumental noise.

To improve the signal-to-noise ratio, the spectra of 1-day segments were stacked over all the stations and over 3 months (90 days); the resultant spectrum was regarded as the average spectrum for the middle of the month. We pasted up these monthly spectra with respect to time to obtain a spectrogram (a contour plot of PSD on the frequency-time plane). The observed modes on the spectrogram (Fig. 1), especially the fundamental spheroidal mode of angular degree 29 (${}_0S_{29}$) and ${}_0S_{37}$, show an annual variation of intensity. This annual variation, however, may not be due purely to the variation of modal amplitudes but be due in part to the variation of the noise level with the modal peaks on it. To estimate the net annual variation of the modal amplitudes, we fitted a parameterized spectral model (*5*) to each spectrum. The model consists of the theoretical free oscillation spectra at peak frequencies of the preliminary reference Earth model (PREM) (*10*), a term originating from atmospheric attraction (*11*), and a linear term simulating the remaining noise. By minimizing the squared difference between the observed and theoretical spectra, we determined the amplitudes of the modes from ${}_0S_{20}$ to ${}_0S_{45}$, including their solution errors (Fig. 2A). Because the annual variation of ${}_0S_{29}$ is larger than those of the other modes, we plotted the amplitude of ${}_0S_{29}$ and the mean amplitude of the other modes separately as a function of month. There are significant annual variations of modal amplitudes beyond their solution errors for ${}_0S_{29}$ and the other modes (Fig. 2). We also computed the average monthly spectrum by stacking the spectra of 1-day segments over all the stations and over the same months of the 9-year period. We fit a parameterized spectral model to each of these averaged monthly spectra by the same method as before (Fig. 2B). The amplitude of ${}_0S_{29}$ shows an annual variation of about 40%, whereas the mean amplitude of the other modes shows a variation of about 10%.

The modes of ${}_0S_{29}$ and ${}_0S_{37}$ are of greater intensities than the other modes (Fig. 1), and these are the modes that can couple with the atmospheric acoustic modes (*12–14*). To quantify this point, we stacked the spectra of 1-day segments over all the stations and over all the periods. We fitted a parameterized spectral model to the resultant spectrum by the same method as before to determine the

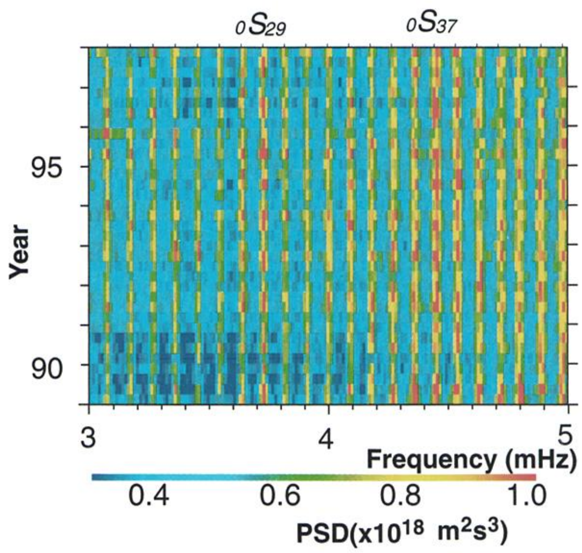

Fig. 1. Spectrogram of the seismically quiet days from 1989 to 1998, which consists of the successive monthly spectra, each of which is an average of the 1-day spectra over 90 days and over all the available stations. This figure blows up the result in a relatively narrow frequency range from 3 to 5 mHz. The vertically intense lines with approximately regular intervals correspond to the spectral peaks of fundamental spheroidal modes, whose theoretical frequencies are indicated by tick marks on the upper edge. The apparent annual variation is observed.

[1]Earthquake Research Institute, University of Tokyo, 1-1-1 Yayoi, Bunkyo-ku, Tokyo 113-0032, Japan. [2]Earth and Planetary Sciences, Tokyo Institute of Technology, 2-12-1 O-okayama, Meguro-ku, Tokyo 152-8550, Japan.

modal amplitudes accurately (Fig. 3). The modal amplitude in general increases with increasing degree from 15 to 45, with two local extrema at degrees 29 and 37. The excess amplitudes of ${}_0S_{29}$ and ${}_0S_{37}$ are on the orders of 20 and 10%, respectively, and are beyond their solution errors. The modes at degrees above 55 and below 15 are poorly resolved (*5*).

Preferential excitation of the seismic modes that can couple atmospheric acoustic modes has been reported. For example, Rayleigh waves with particular periods of about 230 and 270 s were observed to be associated with the 1991 volcanic eruption of Mount Pinatubo (*15, 16*). This observation has been interpreted as a consequence of the continuous thermal energy flux from the volcano that set off the long-wavelength standing acoustic waves in the low-sound-velocity channel of the atmosphere. These acoustic waves in turn excited seismic Rayleigh waves at periods around 230 and 270 s, where atmospheric acoustic waves have about the same horizontal wavelengths as those of Rayleigh waves. This observation has also been interpreted in terms of normal mode theory (*12, 13*), according to which the Rayleigh waves at periods around 270 s correspond to the fundamental spheroidal mode ${}_0S_{29}$ that is coupled with a mode along the fundamental branch of atmospheric acoustic modes, and the 230-s Rayleigh wave corresponds to the ${}_0S_{37}$ mode that is coupled with a mode along the first overtone branch. Thus, our observation of the excess excitations of ${}_0S_{29}$ and ${}_0S_{37}$ (Fig. 3) implies that the acoustic free oscillations are also generated incessantly in the atmosphere in resonance with the background free oscillations of the solid Earth through the two narrow windows at periods around 230 and 270 s. We also note that the excess amplitudes of the mode are only 10 to 20% of the total amplitudes of the adjacent modes. Because the eigenfunction of an acoustic mode increases rapidly with increasing altitude, an atmospheric source at an altitude more than a few kilometers should excite the coupled modes of ${}_0S_{29}$ and ${}_0S_{37}$ preferentially among other modes, just as in the case of the excitation by the eruption of Mount Pinatubo. The observed small excess amplitudes of ${}_0S_{29}$ and ${}_0S_{37}$ indicate that the excitation source lies at or just above Earth's surface.

The annual variation of Earth's background free oscillations also indicates that the excitation source is of atmospheric or oceanic origin rather than in the solid Earth. The amplitudes of the uncoupled modes vary annually by about 10%, with their peaks occurring in July to August, that is, in the summer of the Northern Hemisphere (Fig. 2). Such a variation is relevant to the global average of the outgoing infrared flux from Earth (*17, 18*) (see Fig. 2). The infrared flux is greatest in the summer and least in the winter for the Northern and Southern hemispheres, but with different magnitudes in each. In the Southern Hemisphere, the seasonal effect is moderated by oceans more efficiently than in the Northern Hemisphere. The net result is about a 5% annual variation of the global average of infrared flux, with its maximum occurring in the summer of the Northern Hemisphere. The outgoing infrared flux is a measure of how effectively the warmed air is carried upward to the top of the atmosphere by convective turbulent motions, which should induce dynamic pressure on the surface of the solid Earth. The coincidence of the annual variation of the oscillation amplitudes with the global average of the infrared flux implies that it is this dynamic pressure of atmospheric origin that excites Earth's free oscillations (*4, 6*). The coincidence extends in phase (with the maximum in the summer of the Northern Hemisphere) and in relative amplitude (10% of the total excitation amplitude versus 5% of the infrared flux), with a noticeable exception for the coupled modes, especially for ${}_0S_{29}$, which shows a 40% annual variation, about four times larger than those of the uncoupled modes. For the coupled modes, the modal

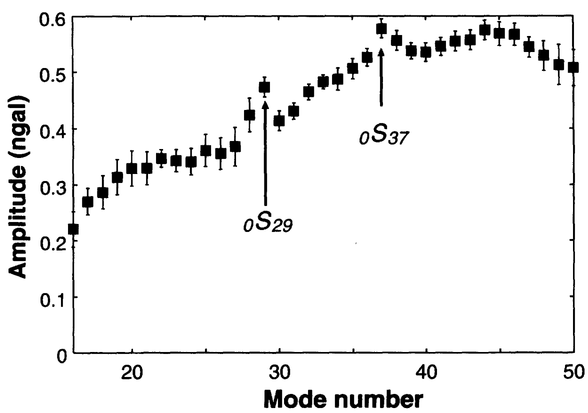

Fig. 3. Amplitudes of the fundamental spheroidal modes averaged over all the available stations and over all the available days from 1989 to 1998. The amplitudes of the coupled modes ${}_0S_{29}$ and ${}_0S_{37}$ are significantly larger than those of the adjacent modes. Error bars indicate the fitting errors.

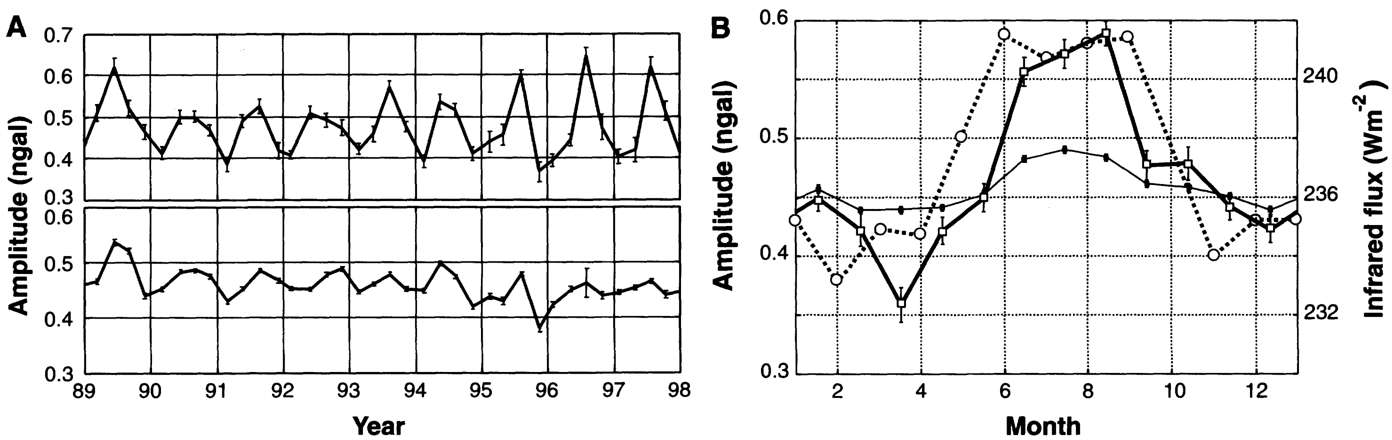

Fig. 2. (**A**) Quarter-annual plots of the modal amplitude of ${}_0S_{29}$ (upper panel) and the mean of those of the other modes from ${}_0S_{20}$ to ${}_0S_{45}$ (lower panel) in a period from 1989 to 1998. Both plots clearly show an annual variation. The amplitude of a mode is calculated from the corresponding spectrum (Fig. 1) by fitting the parameterized spectral model to the observed spectrum. The error bars indicate the fitting errors. (**B**) Annual variations of the modal amplitude of ${}_0S_{29}$ (open squares and thick solid line) and the mean of those of the other modes from ${}_0S_{20}$ to ${}_0S_{45}$ (solid squares and thin solid line) stacked over the whole period from 1989 to 1998. Error bars indicate the fitting errors. The amplitude of the variation is approximately 40% for ${}_0S_{29}$ and 10% for the other modes. Also shown is the global average of infrared flux at the top of the atmosphere in 1994 (*18*) (circles and dashed line), showing an annual variation of about 5%.

energy of acoustic free oscillations will be in part transfered to the resonant modes of seismic free oscillations to amplify the latter amplitudes. This amplification should depend critically on how close the resonant frequencies are between the solid Earth and the atmosphere. The eigenfrequencies of acoustic modes are sensitive to the acoustic structure of the atmosphere (*12*), which varies annually (*19*). The above difference between ${}_0S_{29}$ and other modes suggests that this annual variation of the acoustic structure more precisely tunes the resonant frequencies of acoustic modes to those of seismic modes in the summer of the Northern Hemisphere. We may alternatively attribute the annual variation of the oscillations to the variation of the source height, to which the excitation of coupled modes is sensitive. Thus, the observed phenomena are best explained by the atmospheric excitation hypothesis, although other possibilities, such as disturbances of oceanic origin, cannot be ruled out.

The phenomenon of the background free oscillations represents the hum of the solid Earth, which we found to be resonant with the hum of the atmosphere through the two frequency windows. The excitation source of the hum may be at lowest part of the convective zone of the troposphere, so that it is also responsible for the hum of the atmosphere. The hum in the resonant windows is louder and shows a greater annual variation. The phenomenon can be understood only if the two systems of the solid Earth and atmosphere are viewed as a coupled system.

References and Notes

1. K. Nawa *et al.*, *Earth Planet. Space* **50**, 3 (1998).
2. N. Suda, K. Nawa, Y. Fukao, *Science* **279**, 2089 (1998).
3. T. Tanimoto, J. Um, K. Nishida, N. Kobayashi, *Geophys. Res. Lett.* **25**, 1553 (1998).
4. N. Kobayashi and K. Nishida, *Nature* **395**, 357 (1998).
5. K. Nishida and N. Kobayashi, *J. Geophys. Res.* **104**, 28741 (1999).
6. N. Kobayashi and K. Nishida, *J. Phys. Condens. Matter* **10**, 11557 (1998).
7. S. W. Smith, *Eos* **67**, 213 (1986).
8. G. Roult and J. P. Montagner, *Ann. Geofis.* **37**, 1054 (1994).
9. The 17 IRIS stations we analyzed were AAK (Ala Archa, Kyrgyzstan), BFO (Black Forest, Germany), COL (College Outpost, AK, USA), COR (Corvallis, OR, USA), CTAO (Charters Towers, Australia), ENH (Enshi, China), ESK (Eskdalemuir, Scotland), HIA (Hailar, China), KMI (Kunming, China), LSA (Lhasa, China), MAJO (Matsushiro, Japan), MDJ (Mudanjiang, China), PFO (Pinon Flat, CA, USA), SSE (Shanghai, China), SUR (Sutherland, Republic of South Africa), TLY (Talaya, Russia), and WMQ (Urumqi, China). The eight GEOSCOPE stations were CAN (Mount Stromlo, Canberra, Australia), HYB (Hyderabad, India), INU (Inuyama, Japan), KIP (Kipapa, HI, USA), NOUC (Port Laguerra, Nouvelle Caledonia), SCZ (Santa Cruz, CA, USA), TAM (Tamanrasset, Algeria), and WUS (Wushi, China).
10. A. M. Dziewonski and D. L. Anderson, *Phys. Earth Planet. Inter.* **25**, 297 (1981).
11. D. C. Agnew and J. Berger, *J. Geophys. Res.* **83**, 5420 (1978).
12. S. Watada, thesis, California Institute of Technology, Pasadena, CA (1995).
13. P. Lognonné, E. Clévédé, H. Kanamori, *Geophys. J. Int.* **135**, 388 (1998);
14. P. Lognonné, B. Mosser, F. A. Dahlen, *Icarus* **110**, 186 (1994).
15. H. Kanamori and J. Mori, *Geophys. Res. Lett.* **19**, 721 (1992).
16. R. Widmer and W. Zürn, *Geophys. Res. Lett.* **19**, 765 (1992).
17. H. Jacobowitz *et al.*, *J. Geophys. Res.* **89**, 4997 (1984).
18. R. Kandel *et al.*, *Bull. Am. Meteorol. Soc.* **79**, 765 (1998).
19. E. L. Fleming, S. Chandra, J. J. Barnett, M. Corney, *Adv. Space Res.* **10**, 11 (1990).
20. We are grateful to a number of people who were associated with IRIS and GEOSCOPE. We thank N. Suda, K. Nawa, K. Nakajima, and S. Watada for comments on this paper.

11 November 1999; accepted 8 February 2000

Simulation of Early 20th Century Global Warming

Thomas L. Delworth* and Thomas R. Knutson

The observed global warming of the past century occurred primarily in two distinct 20-year periods, from 1925 to 1944 and from 1978 to the present. Although the latter warming is often attributed to a human-induced increase of greenhouse gases, causes of the earlier warming are less clear because this period precedes the time of strongest increases in human-induced greenhouse gas (radiative) forcing. Results from a set of six integrations of a coupled ocean-atmosphere climate model suggest that the warming of the early 20th century could have resulted from a combination of human-induced radiative forcing and an unusually large realization of internal multidecadal variability of the coupled ocean-atmosphere system. This conclusion is dependent on the model's climate sensitivity, internal variability, and the specification of the time-varying human-induced radiative forcing.

Confidence in the ability of climate models to make credible projections of future climate change is influenced by their ability to reproduce the observed climate variations of the 20th century, including the global warmings in both the early and latter parts of the century (*1*). Several climate models accurately simulate the global warming of the late 20th century when the radiative effects of increasing levels of human-induced greenhouse gases (GHGs) and sulfate aerosols are taken into account (*2–4*). However, the warming in the early part of the century has not been well simulated using these two climate forcings alone. Factors which could contribute to the early 20th century warming include increasing GHG concentrations, changing solar and volcanic activity (*4–6*), and internal variability of the coupled ocean-atmosphere system. The relative importance of each of these factors is not well known.

Here, we examine results from a set of five integrations of a coupled ocean-atmosphere model forced with estimates of the time-varying concentrations of GHGs and sulfate aerosols over the period 1865 to the present, along with a sixth (control) integration with constant levels of greenhouse gases and no sulfate aerosols. In one of the five GHG-plus-sulfate integrations, the time series of global mean surface air temperature provides a remarkable match to the observed record, including the global warmings of both the early (1925–1944) and latter (1978 to the present) parts of the century. Further, the simulated spatial pattern of warming in the early 20th century is broadly similar to the observed pattern of warming. Thus, we demonstrate that an early 20th century warming, with a spatial and temporal structure similar to the observational record, can arise from a combination of internal variability of the coupled ocean-atmosphere system and human-induced radiative forcing from GHG and sulfate aerosols. These results suggest a possible mechanism for the observed early 20th century warming.

The coupled ocean-atmosphere model that was used, developed at the GFDL, is higher in spatial resolution than an earlier version used in many previous studies of climate variability and change (*7, 8*), but it employs similar physics. The coupled model is global in domain and consists of general circulation models of the atmosphere (R30 resolution, corresponding to 3.75° longitude by 2.25° latitude, with 14 vertical levels) and ocean (1.875° longitude by 2.25° latitude, with 18 vertical levels). The model atmosphere and ocean communicate through fluxes of heat, water, and momentum at the air-sea interface. Flux adjustments are used to facilitate the simulation of a realistic mean state. A thermodynamic sea-ice model is used over oceanic regions, with ice movement determined by ocean currents.

Geophysical Fluid Dynamics Laboratory (GFDL)/National Oceanic and Atmospheric Administration, Princeton, NJ 08542, USA.

*To whom correspondence should be addressed. E-mail: td@gfdl.gov